

Crossing the Simulation-Experiment Gap: Style Translation for Enhanced Atomic Structure Discovery from AFM Images

Jie Huang

Surfaces and Interfaces at the Nanoscale (SIN), School of Science, Aalto University, Finland



Surfaces and Interfaces
at the Nanoscale (SIN)

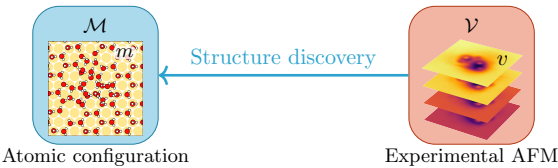
A'' Aalto University
School of Science

Forward mapping from samples to experimental images



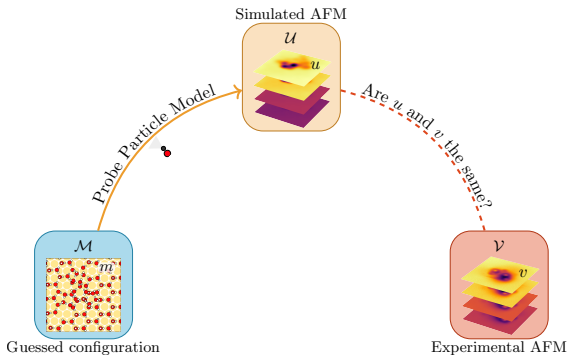
Non-contact atomic force microscopy (NC-AFM) allows us to characterise nanoscale structures. We **realise the mapping from samples to AFM images**, $\mathcal{M} \rightarrow \mathcal{V}$.

Inverse mapping from AFM images to atomic structures



What we want to know the atomic structure through the AFM images.
But it is **challenging** to extract this information directly from the images, $\mathcal{V} \rightarrow \mathcal{M}$.

Structure discovery with DFT and AFM simulations



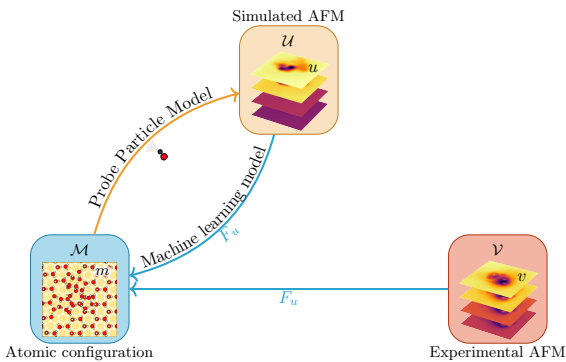
The configuration is guessed using Density Functional Theory (**DFT**). AFM images are simulated by the Probe Particle Model (**PPM**)¹²³. A match with experimental images supports the guessed structure.

¹Hapala, P. et al., *Phys. Rev. B*, 2014, 90(8), 085421. DOI: 10.1103/physrevb.90.085421.

²Hapala, P. et al., *Phys. Rev. Lett.*, 2014, 113(22), 226101. DOI: 10.1103/physrevlett.113.226101

³Oinonen, N. et al., *Comput. Phys. Commun.*, 2024, 305, 109341. DOI: 10.1016/j.cpc.2024.109341

Structure discovery with machine learning



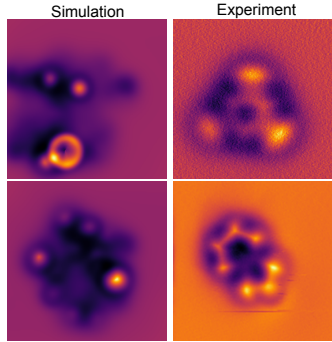
Structure discovery models⁴⁵⁶ learn the inverse map. It's used for **both simulated and experimental** AFM images.

⁴Oinonen, N. et al., *MRS Bulletin*, 2022, 47(9), 895-905. DOI: 10.1557/s43577-022-00324-3.

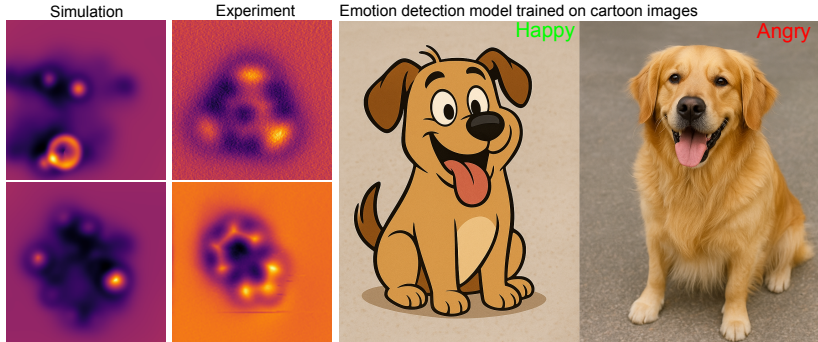
⁵Kurki, L. et al., *ACS Nano*, 2024, 18(17), 11130-11138. DOI: 10.1021/acsnano.3c12654.

⁶Priante, D. et al., *ACS Nano*, 2024, 18(1), 1234-1245. DOI: 10.1021/acsnano.3c10958

Problem: distribution shift and performance degradation

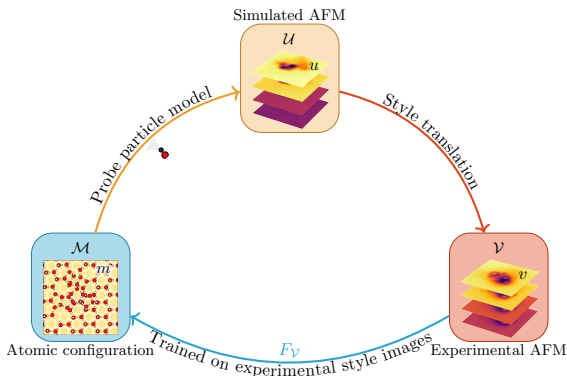


Problem: distribution shift and performance degradation



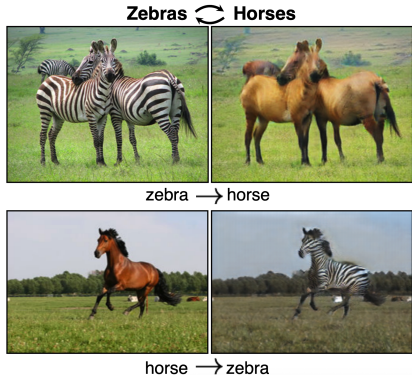
This **style gap** leads to performance decrease when predicting experimental AFM images.

Motivation: How can we improve AFM structure discovery?

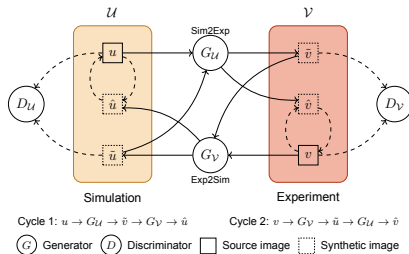
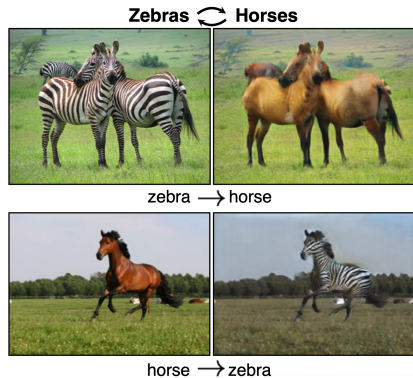


Experiment data can be used for training **is insufficient**. We **translate** the simulated AFM images **to the experimental style** images. Then we use the translated images to train the models.

Method: style translation between image domains



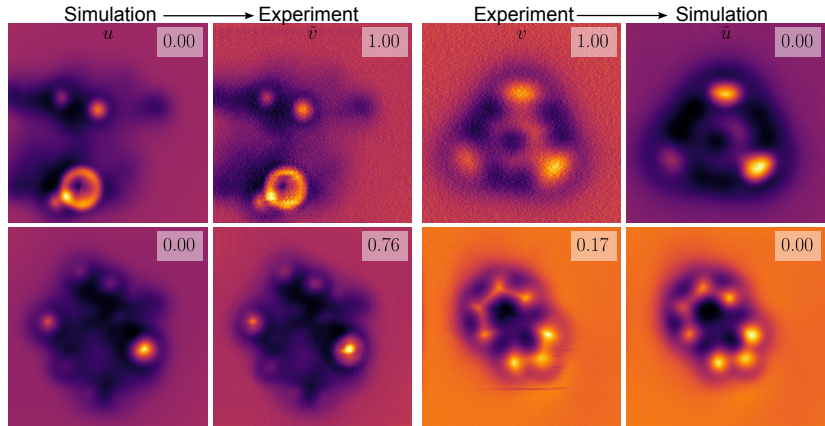
Method: style translation between image domains



- CycleGAN^a learns to map between domains **without paired training data**.

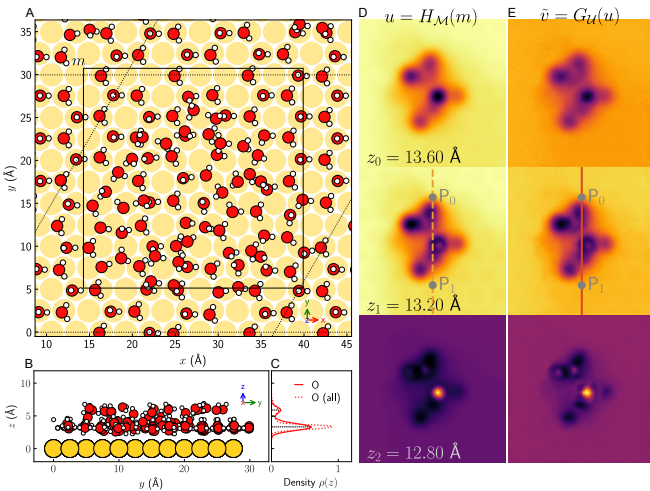
^aZhu, J.-Y. et al., 2020, arXiv:1703.10593

Style translation between simulated and experimental AFM images



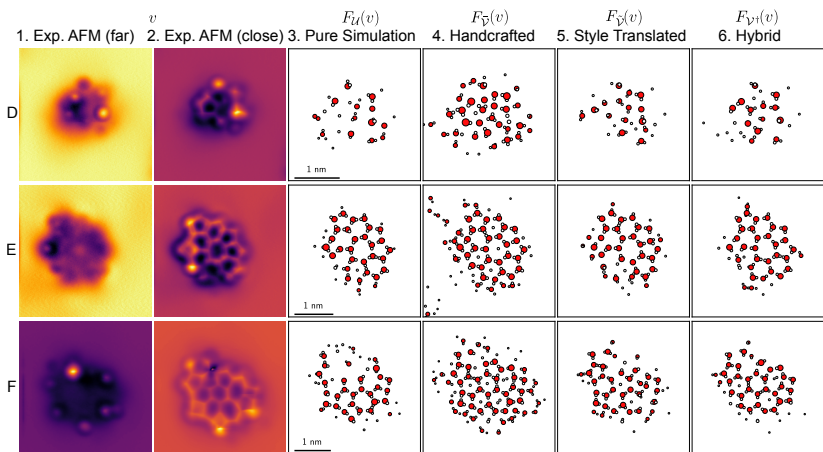
Forward translation can **add** features such as **background noise**, while backward translation can help remove noise and artifacts.

Constructing new training data with style-translated AFM images



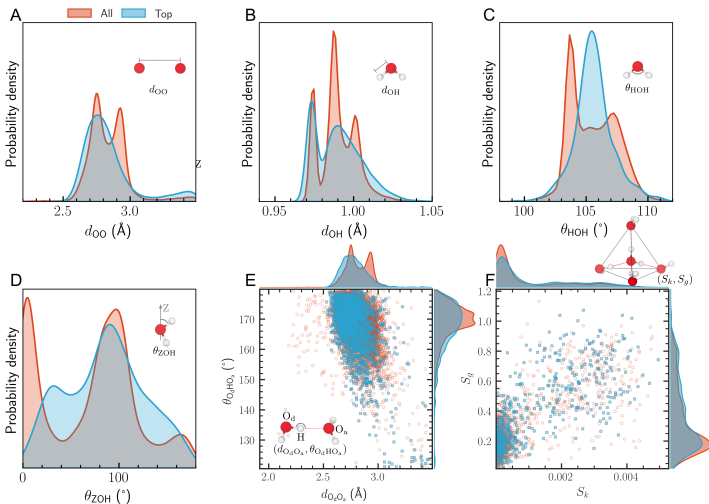
Features are added to simulated images of bi-layer water molecules on Au(111). Experimental-style AFM images with corresponding atomic configurations are used for training.

Atomic structure prediction from experimental AFM images



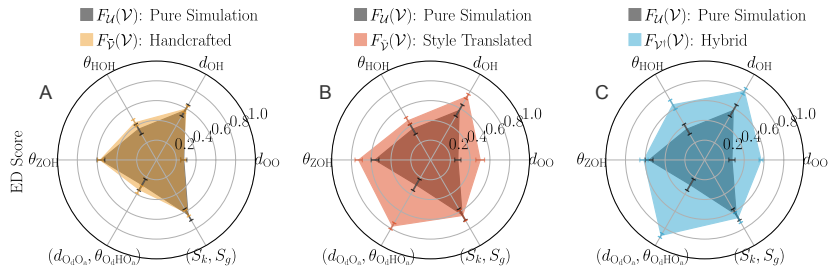
Structure predictions given by models trained on different images data.
Which model is more reliable?

Theoretical local structural distributions obtained from simulations



Good predictions of atomic structures should be consistent with the theoretical local structural distributions.

Performance evaluation based on the theoretical structural distributions



We use the **distribution distances** between the prediction and the theoretical distributions as a metric to evaluate the model performance. Training utilising style translation can lead to significant performance improvements.

Summary and outlook

- **Motivation:** To make structure discovery from AFM images more reliable, especially in **real experimental data**.

Summary and outlook

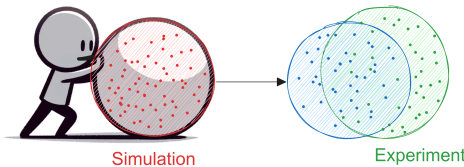
- **Motivation:** To make structure discovery from AFM images more reliable, especially in **real experimental data**.
- **Belief:** Machine learning can help us to achieve this goal, but only if it learns from the **right data**.

Summary and outlook

- **Motivation:** To make structure discovery from AFM images more reliable, especially in **real experimental data**.
- **Belief:** Machine learning can help us to achieve this goal, but only if it learns from the **right data**.
- **Obstacle:** We still can't directly train on experimental images, due to the **lack of sufficient labeled data**.

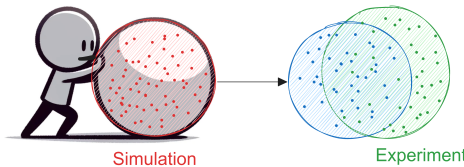
Summary and outlook

- **Motivation:** To make structure discovery from AFM images more reliable, especially in **real experimental data**.
- **Belief:** Machine learning can help us to achieve this goal, but only if it learns from the **right data**.
- **Obstacle:** We still can't directly train on experimental images, due to the **lack of sufficient labeled data**.
- **Approach:** Simulated AFM images → Experimental-style AFM images → Improvements in ML training → Reliable predictions.



Summary and outlook

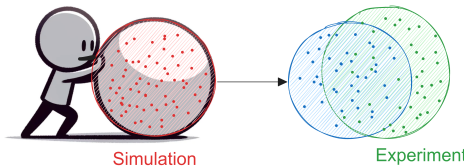
- **Motivation:** To make structure discovery from AFM images more reliable, especially in **real experimental data**.
- **Belief:** Machine learning can help us to achieve this goal, but only if it learns from the **right data**.
- **Obstacle:** We still can't directly train on experimental images, due to the **lack of sufficient labeled data**.
- **Approach:** Simulated AFM images → Experimental-style AFM images → Improvements in ML training → Reliable predictions.



- **Value:** A step closer to the **automated structure discovery**.

Summary and outlook

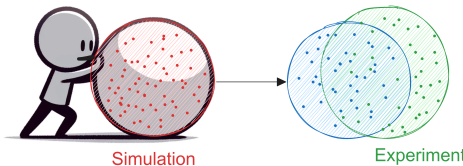
- **Motivation:** To make structure discovery from AFM images more reliable, especially in **real experimental data**.
- **Belief:** Machine learning can help us to achieve this goal, but only if it learns from the **right data**.
- **Obstacle:** We still can't directly train on experimental images, due to the **lack of sufficient labeled data**.
- **Approach:** Simulated AFM images → Experimental-style AFM images → Improvements in ML training → Reliable predictions.



- **Value:** A step closer to the **automated structure discovery**.
- **Limitation:** Finding the right parameter for style translation takes time.

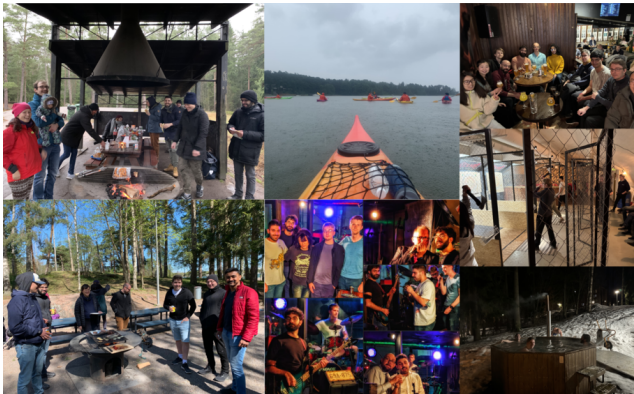
Summary and outlook

- **Motivation:** To make structure discovery from AFM images more reliable, especially in **real experimental data**.
- **Belief:** Machine learning can help us to achieve this goal, but only if it learns from the **right data**.
- **Obstacle:** We still can't directly train on experimental images, due to the **lack of sufficient labeled data**.
- **Approach:** Simulated AFM images → Experimental-style AFM images → Improvements in ML training → Reliable predictions.



- **Value:** A step closer to the **automated structure discovery**.
- **Limitation:** Finding the right parameter for style translation takes time.
- **Outlook:** A more advanced probe particle model, and automatic workflow.

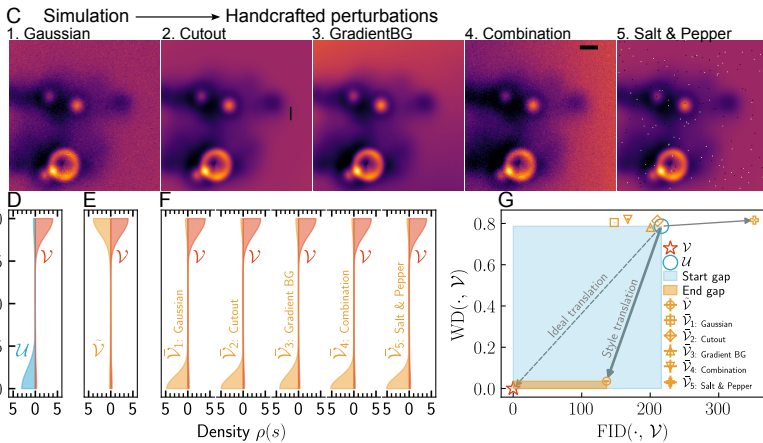
Acknowledgements



SIN group in Aalto University, Finland.

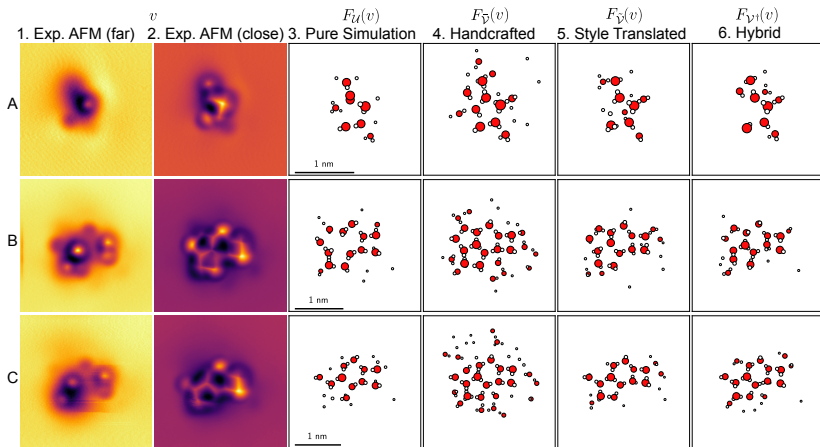
- Niko Oinonen, Fabio Priante, Filippo Federici Canova, Lauri Kurki, and Adam S. Foster.
- PPM: <https://github.com/Probe-Particle/ppafm>
- Prof. Ying Jiang's lab, Peking University, China.
- World Premier International Research Center Initiative (WPI), MEXT, Japan.
- The Academy of Finland (Projects 347319 and 346824).
- Computational resources provided by the Aalto Science-IT Project and CSC.

Style translation evaluation



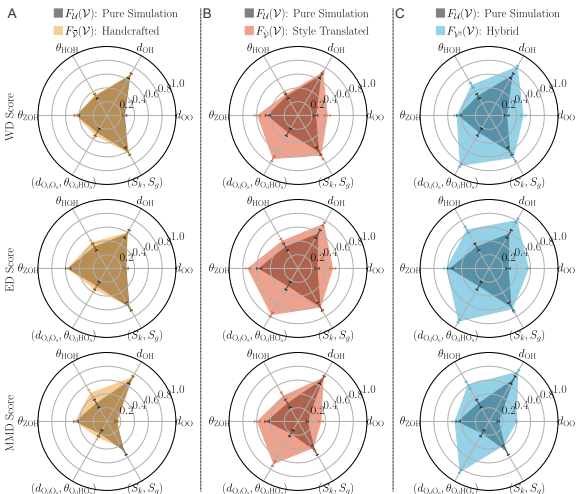
Style translation can be used to **reduce the style gap** between simulation and experimental AFM images.

Atomic structure predictions from experimental AFM images: smaller clusters



We train models on different AFM images and use them to predict the atomic structure from the experimental AFM images.

Performance evaluation based on the theoretical structural distributions



We use the Wasserstein distance between the prediction and the theoretical distributions as a metric to evaluate the model performance.

Translational tetrahedral order S_k

The translational tetrahedral order S_k is defined as

$$S_k = \frac{1}{3} \sum_{k=1}^4 \frac{(r_k - \bar{r})^2}{4\bar{r}^2}, \quad (1)$$

where r_k is the radial distance from the central oxygen atom to the k -th peripheral oxygen atom, and \bar{r} is the arithmetic mean of the four radial distances. This parameter quantifies the variance in radial distances, with $S_k = 0$ for a perfect tetrahedron and increasing as the structure becomes distorted.

Orientational tetrahedral order S_g

The orientational tetrahedral order S_g is defined as

$$S_g = \frac{3}{8} \sum_{j=1}^3 \sum_{k=j+1}^4 \left(\cos \psi_{j,k} + \frac{1}{3} \right)^2 \quad (2)$$

where $\psi_{j,k}$ is the angle between bonds j and k at the central oxygen. A perfect tetrahedron yields $S_g = 0$, while random angular arrangements yield an average $\langle S_g \rangle \approx 1$ due to the normalisation factor. Each point in the distribution corresponds to a local environment consisting of a central oxygen atom and its four nearest neighbours within a 3.5 Å cutoff.

Wasserstein distance

Wasserstein distance (also called Earth Mover's distance) is a measure of the dissimilarity between two distributions. Intuitively, it quantifies the minimum "effort" required to transform one distribution into another, where the effort is measured by the amount of probability mass that must be transported and the distance it must be moved. Mathematically, the Wasserstein distance between two distributions X, Y is defined as follows:

$$\begin{aligned} \text{WD}(X, Y) &= \inf_{\pi \in \Pi(X, Y)} \int_{\mathbb{R} \times \mathbb{R}} \|x - y\| d\pi(x, y) \\ &= \inf_{\pi \in \Pi(X, Y)} \mathbb{E}_{(x, y) \sim \pi} [\|x - y\|]. \end{aligned} \tag{3}$$

Here, $\Pi(X, Y)$ denotes the set of all joint distributions $\pi(x, y)$ whose marginals are respectively X and Y . The joint distribution $\pi(x, y)$ specifies a transport plan indicating how much mass should be transported from x to y . The Wasserstein distance is then the minimum cost of the transport plan.



FID

Fréchet inception distance (FID) was first introduced to evaluate the performance of GAN models. The FID between two image distributions X and Y is computed as follows. Collect image samples $x_1, \dots, x_m, y_1, \dots, y_n$ from X, Y , respectively. Encode all samples x_i and y_i by computing the activations $A(x_i)$ and $A(y_i)$ of the final layer of the pretrained Inception network. Compute the sample means μ_1, μ_2 and the sample covariance matrices Σ_1, Σ_2 of the activations $A(x_i), A(y_i)$. The FID is the WD between the two multivariate normal distributions $N(\mu_1, \Sigma_1)$ and $N(\mu_2, \Sigma_2)$.

$$\text{FID}(X, Y) = \|\mu_1 - \mu_2\|_2^2 + \text{tr}(\Sigma_1) + \text{tr}(\Sigma_2) - 2 \cdot \text{tr} \left(\sqrt{\Sigma_1 \Sigma_2} \right) \quad (4)$$

Maximum mean discrepancy

Maximum mean discrepancy (MMD) is another distance measurement between random variables X and Y , which is defined as the distance between their embeddings in the reproducing kernel Hilbert space (RKHS). MMD quantifies the dissimilarity between two distributions by comparing their mean representations in a high-dimensional feature space. Given two probability distributions X and Y , the MMD between them is defined as follow:

$$\text{MMD}(X, Y) = \|\mu_X - \mu_Y\|_{\mathcal{H}}, \quad (5)$$

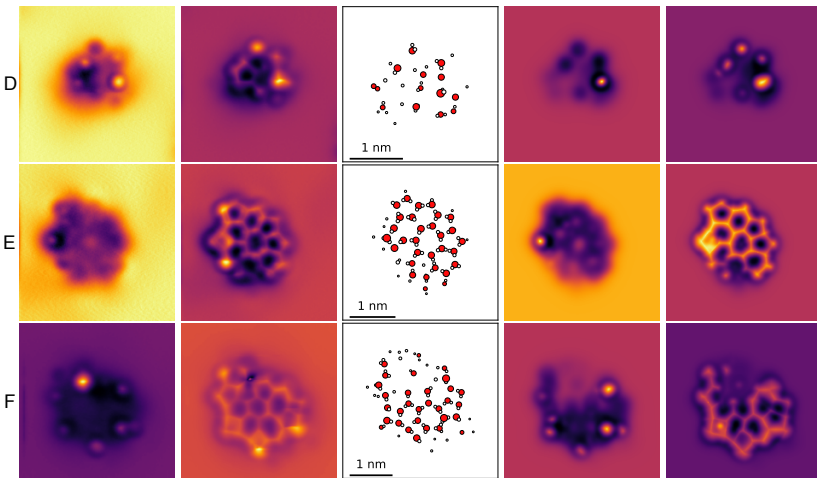
where μ_X, μ_Y are the mean embeddings of X and Y in RKHS \mathcal{H} . We calculate the empirical estimation of MMD through

$$\begin{aligned} \text{MMD}^2(X, Y) &= \left\| \frac{1}{n} \sum_{i=1}^n \varphi(x_i) - \frac{1}{m} \sum_{i=1}^m \varphi(y_i) \right\|_{\mathcal{H}}^2 \\ &= \frac{1}{n^2} \sum_{i=1}^n \sum_{j=1}^n k(x_i, x_j) + \frac{1}{m^2} \sum_{i=1}^m \sum_{j=1}^m k(y_i, y_j) \\ &\quad - \frac{2}{nm} \sum_{i=1}^n \sum_{j=1}^m k(x_i, y_j), \end{aligned} \quad (6)$$

where kernel $k(x, y)$ is a function that measures the similarity between two data points x and y . We use the Gaussian kernel: $k(x, y) = \exp(-\|x - y\|^2/(2\sigma^2))$, where σ is the bandwidth parameter.

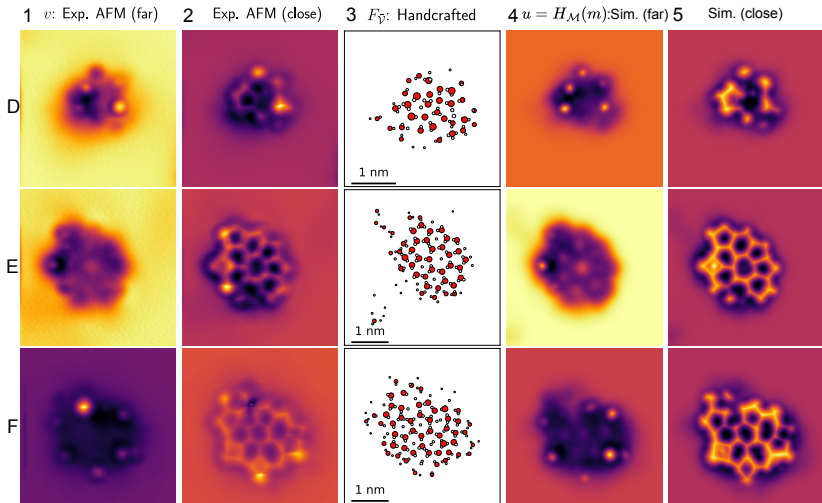
PPM simulations for the predicted structures: Pure simulation

1 v : Exp. AFM (far) 2 Exp. AFM (close) 3 $F_U(v)$: Pure Simulation 4 $u = H_{\mathcal{M}}(m)$: Sim. (far) 5 Sim. (close)



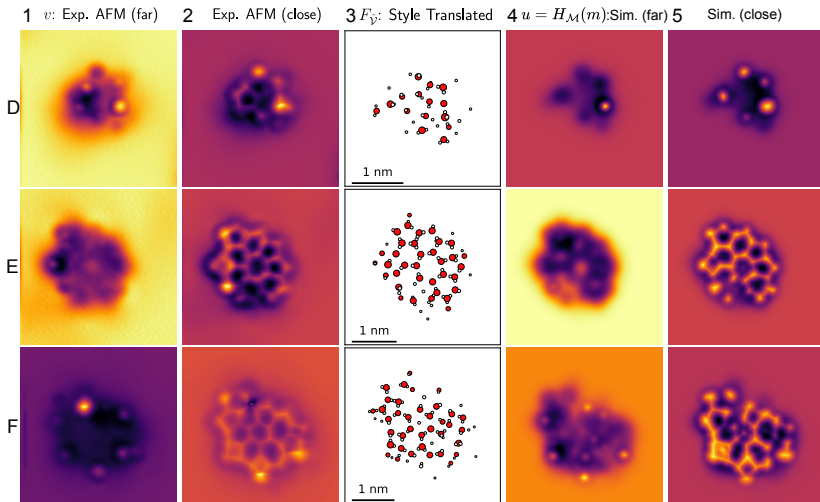
Inputs, predictions, and recovered PPM simulations.

PPM simulations for the predicted structures: Handcrafted perturbations



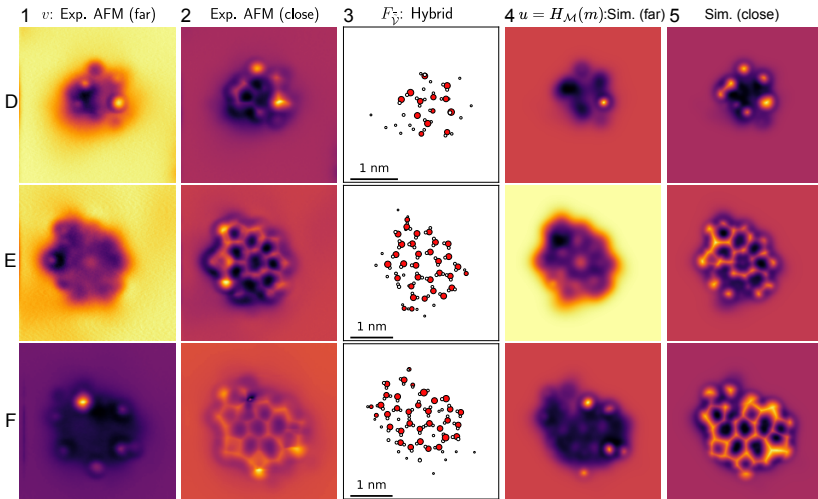
Inputs, predictions, and recovered PPM simulations.

PPM simulations for the predicted structures: Style translation



Inputs, predictions, and recovered PPM simulations.

PPM simulations for the predicted structures: Hybrid



Inputs, predictions, and recovered PPM simulations.

Experiment details

- 5 K using qPlus sensors
- Spring constant $k_0 = 1800 \text{ N/m}$, resonances frequencies of $f_0 = 29.1 \text{ kHz}$, and quality factor $Q = 10^5$
- AFM frequency shift (Δf) images were obtained with the CO-terminated tips in constant-height mode